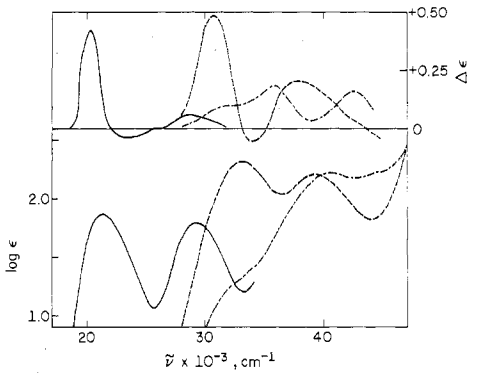

Figure 3. Electronic absorption (lower part) and circular dichroism (upper part) of 1,2-[$(+)^{CD}_{492}$-$Co(en)_2(NH_3)_2]^{3+}$ (—), 1,2-[$(+)^{CD}_{325}$-$Rh(en)_2(NH_3)_2]^{3+}$ (– – –), and 1,2-[$(+)^{CD}_{280}$-$Ir(en)_2(NH_3)_2]^{3+}$ (– – –). The data for 1,2-[$(+)^{CD}_{492}$-$Co(en)_2(NH_3)_2]^{3+}$ are taken from ref 27 and 28.

The optically active complexes given in Table V form the less-soluble (+)-BCS salts except for the optically active diammine complexes. This also indicates that, from view of the solubility rule,[31] these enantiomers probably have the same absolute configuration.

Whole aspects of the ammoniation reactions of rhodium(III) and iridium(III) complexes studied in this work may suggest that the reactions proceed with complete retention of configuration and all optically active complexes listed in Table V have the Λ configuration.

Acknowledgment. The authors gratefully acknowledge the financial assistance of the National Science Foundation (Grants GP 5318 and GP 9370).

Registry No. 1,6-$[Rh(en)_2Cl_2]Cl$, 15444-63-0; 1,2-$[Rh(en)_2Cl_2]Cl$, 15444-62-9; 1,6-$[Rh(en)_2Br_2]NO_3$, 15529-89-2; 1,2-$[Rh(en)_2Br_2]Br$, 65761-17-3; 1,6-$[Rh(en)_2I_2]I$, 39561-35-8; 1,2-$[Rh(en)_2I_2]I$, 53368-51-7; 1,6-$[Rh(en)_2(NH_3)Cl](NO_3)_2$, 65802-28-0; 1,2-$[Rh(en)_2(NH_3)Cl]Cl_2$, 65794-88-9; 1,6-$[Rh(en)_2(NH_3)Br](NO_3)_2$, 65761-16-2; 1,6-$[Rh(en)_2(NH_3)I]I_2$, 65761-15-1; 1,6-$[Rh(en)_2(NH_3)_2](ClO_4)_3$, 65761-21-9; 1,2-$[Rh(en)_2(NH_3)_2](ClO_4)_3$, 65794-95-8; 1,6-$[Ir(en)_2Cl_2]Cl$, 15444-46-9; 1,2-$[Ir(en)_2Cl_2]Cl$, 15444-47-0; 1,2-$[Ir(en)_2(NH_3)_2](ClO_4)_3$, 65794-93-6; 1,6-$[Co(en)_2(NH_3)_2]Cl_3$, 36883-69-9; 1,2-$[Co(en)_2(NH_3)_2](ClO_4)_3$, 15079-83-1; Λ-1,2-$[Co(en)_2(NH_3)Cl]^{2+}$, 45837-30-7; Λ-1,2-$[Co(en)_2Cl_2]^+$, 18660-62-3; Δ-1,2-$[Co(en)_2Cl_2]^+$, 45837-15-8; Λ-1,2-$[Rh(en)_2(NH_3)_2]^{3+}$, 65794-91-4; Λ-1,2-$[Rh(en)_2(NH_3)Cl]^{2+}$, 65794-90-3; Δ-1,2-$[Rh(en)_2(NH_3)Cl]^{2+}$, 65794-89-0; Λ-1,2-$[Rh(en)_2Cl_2]^+$, 65830-10-6; Λ-1,2-$[Rh(en)_2Br_2]^+$, 65830-11-7; Δ-1,2-$[Rh(en)_2Br_2]^+$, 64598-98-7; Λ-1,2-$[Ir(en)_2(NH_3)_2]^{3+}$, 65830-12-8; Λ-1,2-$[Ir(en)_2Cl_2]^+$, 45838-56-0.

Supplementary Material Available: Figure for infrared spectra of bis(ethylenediamine)diammine complexes of cobalt(III), rhodium(III), and iridium(III) in the NH_2 asymmetric deformation region and figures for ^1H NMR spectra of bis(ethylenediamine) complexes of cobalt(III), rhodium(III), and iridium(III) (3 pages). Ordering information is given on any current masthead page.

References and Notes

(1) Postdoctoral Research Associate, University of Illinois, 1968–1969.
(2) (a) J. C. Bailar, Jr., J. H. Haslam, and E. M. Jones, *J. Am. Chem. Soc.*, **58**, 2226 (1936); (b) R. D. Archer and J. C. Bailar, Jr., *ibid.*, **83**, 812 (1961).
(3) J. C. Bailar, Jr., *Inorg. Synth.* **2**, 222 (1946).
(4) A. Werner and V. L. King, *Ber. Dtsch. Chem. Ges.*, **44**, 1890 (1911).
(5) J. B. Work, Ph.D. Thesis, University of Illinois, 1942, p 44.
(6) A. Werner, *Justus Liebigs. Ann. Chem.*, **351**, 65 (1907).
(7) S. Anderson and F. Basolo, *J. Am. Chem. Soc.*, **82**, 4423 (1960).
(8) S. A. Johnson and F. Basolo, *Inorg. Chem.*, **1**, 925 (1962).
(9) S. Kida, *Bull. Chem. Soc. Jpn.*, **39**, 2415 (1966).
(10) R. A. Bauer and F. Basolo, *Inorg. Chem.*, **8**, 2231 (1969).
(11) In this paper, an optical isomer is designated mainly by $(+)^{CD}_{\lambda}$ or $(-)^{CD}_{\lambda}$, which is the sign of the circular dichroism (CD) curve. The suffix λ represents the wavelength (nm) used for the measurement. In some cases, $(+)^{RD}_{\lambda}$ or $(-)^{RD}_{\lambda}$ is used, where the sign represents the optical rotation at the given wavelength. 1,2-$[(-)^{CD}_{608}$-$Co(en)_2Cl_2]Cl$ correponds to the 1,2-$[(+)^{RD}_{589}$-$Co(en)_2Cl_2]Cl$ isomer.
(12) F. P. Dwyer and F. L. Garvan, *Inorg. Synth.*, **6**, 192 (1960).
(13) H. Ogino, M. Takahashi, and N. Tanaka, *Bull. Chem. Soc. Jpn.*, **43**, 424 (1970).
(14) H. Yoneda and Y. Morimoto, *Bull. Chem. Soc. Jpn.*, **39**, 2180 (1966).
(15) D. A. Buckingham, L. Durham, and A. M. Sargeson, *Aust. J. Chem.*, **20**, 257 (1967).
(16) H. Yoneda and Y. Nakashima, *Bull. Chem. Soc. Jpn.*, **47**, 669 (1974).
(17) D. N. Hendrickson and W. L. Jolly, *Inorg. Chem.*, **9**, 1197 (1970).
(18) H. Yamatera, *Bull. Chem. Soc. Jpn.*, **31**, 95 (1958).
(19) R. A. D. Wentworth and T. S. Piper, *Inorg. Chem.*, **4**, 709, 1524 (1965), and references cited therein.
(20) C. J. Hawkins, "Absolute Configuration of Metal Complexes", Wiley, New York, N.Y., 1971, p 157.
(21) N. Matsuoka, J. Hidaka, and Y. Shimura, *Bull. Chem. Soc. Jpn.*, **40**, 1868 (1967).
(22) C. K. Jørgensen, *Acta Chem. Scand.*, **10**, 500 (1956).
(23) A. J. McCaffery, S. F. Mason, and R. E. Ballard, *J. Chem. Soc.*, 2883 (1965).
(24) K. Matsumoto, S. Ooi, and H. Kuroya, *Bull. Chem. Soc. Jpn.*, **43**, 3801 (1970).
(25) The symbols used here to denote absolute configurations are according to the IUPAC proposal: *Inorg. Chem.*, **9**, 1 (1970).
(26) A. J. McCaffery, S. F. Mason, and B. J. Norman, *J. Chem. Soc.*, 5094 (1965).
(27) A. J. McCaffery, S. F. Mason, and B. J. Norman, *Chem. Commun.*, 132 (1965).
(28) S. F. Mason and B. J. Norman, *Chem. Commun.*, 73 (1965).
(29) Y. Saito, K. Nakatsu, M. Shiro, and H. Kuroya, *Bull. Chem. Soc. Jpn.*, **30**, 795 (1957).
(30) S. K. Hall and B. E. Douglas, *Inorg. Chem.*, **7**, 533 (1968).
(31) A. Werner, *Ber. Dtsch. Chem. Ges.*, **45**, 121, 865 (1912).
(32) T. E. MacDermott and A. M. Sargeson, *Aust. J. Chem.*, **16**, 334 (1963).

Contribution from the Departments of Chemistry, University of Houston, Houston, Texas 77004, and California State University, Fullerton, California 92634

Reactions of Pyridine with a Series of Para-Substituted Tetraphenylporphyrincobalt and -iron Complexes

K. M. KADISH,*[1a] L. A. BOTTOMLEY,[1a,b] and D. BEROIZ

Received August 22, 1977

The effect of substituents on electrode reactions and ligand binding characteristics of para-substituted cobalt and iron tetraphenylporphyrins was investigated by the technique of cyclic voltammetry. The mechanism of electron transfer is discussed, and comparisons are made between the ligand binding reactions of TPPFeCl and TPPCo in several solvents. Equilibrium constants showed either a negative, positive, or zero Hammett relationship depending upon the charge on the central metal and the solvent.

During recent years a number of papers have been published which elucidate linear free energy relationships involving metalloporphyrins. These studies have focused on measuring polarographic half-wave potentials,[2-5] electron-transfer kinetics,[5] porphyrin spectroscopic properties,[6] phenyl ring rotation,[7a] kinetics of ligand exchange,[7b] and stability constants for axial ligand addition to form 1:1 and 2:1 complexes with metalloporphyrins.[3,8-14] It has been shown that the addition

0020-1669/78/1317-1124$01.00/0

of electron-donating or electron-withdrawing groups to the porphyrin ring influence the magnitude of stability constants for Lewis base complexation of the complexes containing cobalt(II),[3] nickel(II),[9,10] vanadyl(II),[10] zinc(II),[11] iron(III),[12-14] and iron(II).[14] These changes in the formation constant as a function of porphyrin ring substituent may be quantitated using the Hammett linear free energy relationship[15]

$$\log K^X/K^H = \Sigma\sigma\rho \quad (1)$$

where K^X is the formation constant for ligand addition to the para- or meta-substituted tetraphenylporphyrin and K^H is the formation constant for the unsubstituted species.

For all complexes containing a +2 central metal, the measured ρ was positive indicating an increased stability of the mono or bis adduct with increasing positive charge on the metal center. However, plots of log K^X/K^H vs. $\sum\sigma$ for an iron(III) complex, (*p*-X)TPPFe(*N*-CH_3Im)$_2$Cl, gave a negative slope of $\rho = -0.39$ in $CHCl_3$.[12] The formation constants were obtained using spectrophotometric techniques. This negative slope was also confirmed by La Mar, who obtained a $\rho = -0.41$ using NMR techniques.[13] The negative sign of ρ was rationalized on the basis of a stabilization of the positively charged (*p*-X)TPP(Fe^{III})$^+$ and there appeared to be a clear indication that stabilization of an ion-paired product, (*p*-X)TPPFe(*N*-CH_3Im)$_2^+Cl^-$, dominated the reactions of (*p*-X)TPPFeCl with axial ligands.

In a recent communication[14] we presented the first comparison between substituent effects on formation of PFe(py)$_2$, PFe(py)$_2^+Cl^-$, and PFe(py)(DMF)$^+Cl^-$ in DMF where py is pyridine and P represents the para- or meta-substituted tetraphenylporphyrin, (*p*-X)TPP^{2-} or (*m*-X)TPP^{2-}. Both iron(III) and iron(II) porphyrins are known to form bis coordination complexes with pyridine,[17] while iron(III) will also form a mono ligand adduct in some solvents.[12] In agreement with the $\rho = -0.39$ to -0.41 obtained for PFe(*N*-CH_3Im)$_2^+Cl^-$ formation in chloroform,[12,13] we obtained a $\rho = -0.433$ for PFe(py)$_2^+Cl^-$ formation in DMF. The reaction constant was also negative for formation of the mono(pyridine) adduct PFe(py)(DMF)$^+Cl^-$. In this case, different values were observed for compounds containing para and meta substituents. Compounds containing para substituents gave a $\rho = -0.454$ while those containing meta substituents gave a $\rho = -0.123$. With the iron(II) complexes a single positive $\rho = 0.127$ was obtained for PFe(py)$_2$ formation.

In this paper we present further results on substituent effects involving metal(II) and metal(III) porphyrins. For a comparison with the iron complexes we have concentrated on the ligand binding reactions of tetraphenylporphyrin complexes of cobalt(II) and cobalt(III). As in the initial communication,[14] stability constants for complex formation were evaluated electrochemically using shifts of polarographic half-wave potentials.

Experimental Section

The para-substituted cobalt tetraphenylporphyrins, (*p*-X)TPPCo, and iron tetraphenylporphyrins, (*p*-X)TPPFeCl, were the generous gift of Dr. F. Ann Walker and Dr. D. G. Davis and were synthesized by the method of Adler et al.[20] Pyridine, py, and dimethyl sulfoxide, Me_2SO ("Spectroquality", MCB), were used without further purification. Tetrabutylammonium perchlorate, TBAP (Southwestern Analytical Lab, Inc.), was recrystallized from methanol and vacuum dried over P_4O_{10} at room temperature. Deaeration was accomplished by passing high-purity nitrogen or argon through the solution for 10 min and blanketing the solution during analysis. All solutions were 0.1 M in TBAP.

Cyclic voltammetric measurements were obtained with a three-electrode system with a PAR Model 174 polarographic analyzer and Houston Instruments Model 2000 recorder or a PAR Model 173 potentiostat, using a PAR Model 175 universal programmer and a storage oscilloscope. The working electrode was a platinum button and a platinum wire served as the auxiliary electrode. A commercial saturated calomel electrode (SCE) was used as the reference electrode and was separated from the bulk of the solution by a fritted glass disk.

Changes in axial coordination upon electron transfer were determined by shifts in polarographic half-wave potential as a function of the ligand concentration. Anodic or cathodic shifts in potential from the uncomplexed species depend on the stoichiometry of the oxidized and reduced complex, the concentration of the free ligand in solution, and the relative magnitudes of the stability constants involving the oxidized and reduced complexes[19]

$$(E_{1/2})_c = (E_{1/2})_s - \frac{0.059}{n}\log\frac{K_{ox}}{K_{red}} - \frac{0.059}{n}\log(L)^{p-q} \quad (2)$$

at 25 °C. $(E_{1/2})_c$ and $(E_{1/2})_s$ are the half-wave potentials of the complexed and uncomplexed oxidized species, respectively; K_{ox} and K_{red} are the formation constants of the oxidized and reduced complexes; (L) is the free concentration of the complexing ligand; p and q are the number of ligands bound to the oxidized and reduced species, respectively, and n is the number of electrons transferred in the diffusion-controlled reaction Ox + $ne \rightleftarrows$ Red.

Half-wave potentials were measured for the M(III) $\rightleftarrows$ M(II) and M(II) $\rightleftarrows$ M(I) reaction in each solvent and during electrochemical titrations with each ligand. The number of electrons transferred was determined by cyclic voltammetry. Plots of $E_{1/2}$ vs. log (ligand) were constructed, and from the slope, the change in coordination number upon reduction was determined using eq 2. Insertion of p and q into this equation yielded the ratio of the formation constants (K_{ox}/K_{red}) for the M(III) complex over the M(II) complex. Independent determination of the M(II) formation constants was accomplished by electrochemically monitoring the further reduction to the +1 metal oxidation state. Since neither cobalt(I) nor iron(I) porphyrins bind nitrogenous bases, the formation constant, K_{red}, and q could be determined directly from the shift of $E_{1/2}$, with the log (L). Insertion of K_{red} into the ratio K_{ox}/K_{red} then enabled us to calculate K_{ox}.

Values of 4σ used in this study were taken from Jaffe.[21] Reaction constants were evaluated by the least-squares best-fit method. Throughout the paper P will be used to represent (*p*-X)TPP^{2-}, where X is an electron-donating or -withdrawing substituent placed at the para position of the four phenyl rings.

Results

Electrode Reactions of (*p*-X)TPPCo. Cyclic voltammograms of (*p*-CH_3)TPPCo in Me_2SO containing various pyridine concentrations are shown in Figure 1. All oxidation–reduction reactions were diffusion-controlled single-electron transfers and corresponded to either the metal-centered oxidation, Co(II) $\rightleftarrows$ Co(III), at 0.2 to −0.2 V or the metal-centered reduction, Co(II) $\rightleftarrows$ Co(I), at −0.8 to −1.0 V.[3] In Figure 1b is shown the transition region between two separate electrode reactions involving different axial coordination of cobalt(III). The transition was observed for all of the investigated para-substituted complexes and appeared in the range of 0.03–0.05 M pyridine. For each complex the transition region consisted of a single oxidation peak and two closely spaced reduction peaks which were coupled to the initial oxidation process.

The half-wave potentials of each reaction were a function of pyridine concentration and shifted cathodically along the potential axis according to the degree of axial complexation. A plot of $E_{1/2}$ vs. log (pyridine) is illustrated in Figure 2 for the electrode reactions of (*p*-CH_3)TPPCo. This figure has been divided into three regions of pyridine concentration on the basis of the prevailing electron-transfer reactions.

In regions A and B, additions of pyridine to (*p*-CH_3)TPPCo produced no changes in the potentials for the (*p*-CH_3)TPPCo $\rightleftharpoons$ (*p*-CH_3)TPPCo$^-$ reduction (identified as process III, Figures 1 and 2). The anodic and cathodic peak separation remained constant with scan rate and $E_{1/2}$ was unchanged from −0.84 V in Me_2SO. In addition, the cathodic peak shape, $|E_p - E_{p/2}|$, was invariant at 0.055 ± 0.005 V indicating the presence of a single electron transfer which is diffusion controlled.[22]

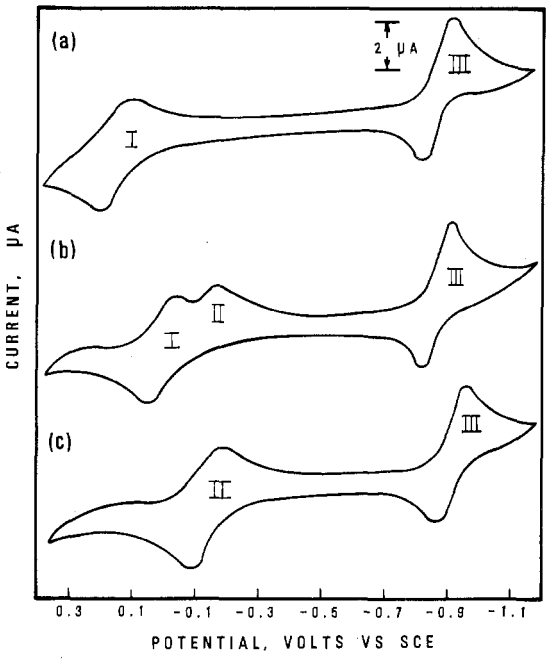

Figure 1. Cyclic voltammograms of (p-CH_3)TPPCo in Me_2SO–pyridine mixtures, containing 0.1 M TBAP (scan rate = 0.060 V/s): (a) neat Me_2SO; (b) 0.03 M pyridine; (c) 1.0 M pyridine.

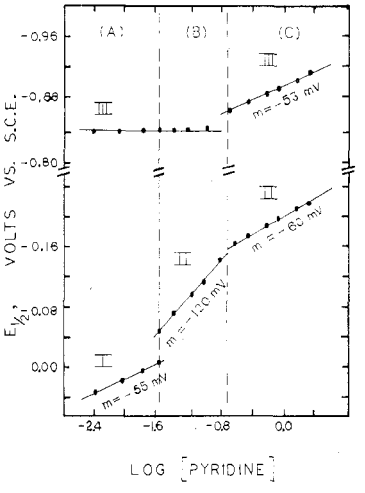

Figure 2. Plot of half-wave potential vs. log (pyridine) for the electrode reactions of (p-CH_3)TPPCo in Me_2SO. Regions A, B, and C refer to the range of pyridine concentrations in which different electrode reactions occur and are explained in text. The Roman numerals I–III correspond to the peaks shown in Figure 1.

The potential for the Co(II) $\rightleftharpoons$ Co(III) reaction shifted cathodically by 55 mV/log (py) in region A and by 120 mV/log (py) in region B. In region B, the peaks for the Co(II) oxidation (process I) disappeared and a new set of peaks appeared about 50 mV more cathodic in potential. These peaks are labeled as process II in Figure 1 and 2.

At pyridine concentrations greater than 0.18 M (region C) potentials of the Co(II) $\rightleftharpoons$ Co(III) and Co(II) $\rightleftharpoons$ Co(I) reactions were both dependent on pyridine concentration. Plots of $E_{1/2}$ vs. log (py) yielded slopes of −60 and −53 mV, respectively. The cathodic peak shape, $|E_p - E_{p/2}|$, was that predicted for a diffusion-controlled one-electron transfer. Similar peak shapes and plots of $E_{1/2}$ vs. log (py) were obtained for all compounds in Me_2SO containing up to 1.0 M pyridine.

Mechanism of (p-X)TPPCo Oxidation–Reduction in Me_2SO. Based on Figure 2 and eq 2, Scheme I is proposed for electrooxidation–reduction of (p-X)TPPCo in Me_2SO–pyridine mixtures where (A), (B), and (C) represent the regions shown

Scheme I

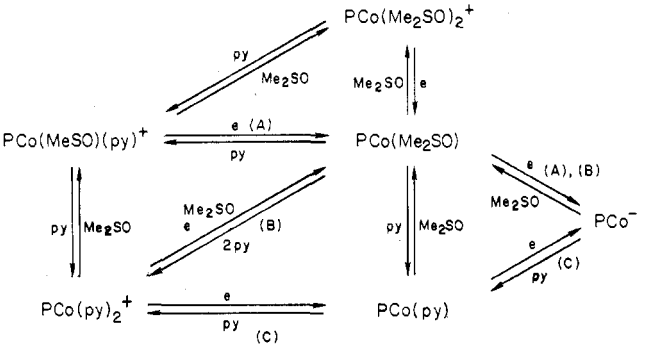

in Figure 2. Parts of the above mechanism are similar to that presented by Truxillo and Davis[18] for reactions of the unsubstituted TPPCo in Me_2SO. Results of spectrophotometric and ESR data on several cobalt(II) porphyrins indicate that five-coordinate complexes are strongly favored.[3,23,24] Assignment of one or two Me_2SO molecules on the axial position of Co(III) is based on the results of electrochemical titrations with Me_2SO and pyridine and is consistent with the preference for six-coordinate complexes.

Scheme I differs significantly from formulations in an earlier study[18] in that we have been able, through judicious selection of pyridine concentration, to isolate the mono(pyridine) adduct of cobalt(III), (p-X)TPPCo(Me_2SO)(py)$^+$. Formation of a mono(pyridine) adduct with Co(III) by electrooxidation of (p-X)TPPCo(Me_2SO) was presumably not observed in earlier studies due to the small range of pyridine concentrations for which it is shown to exist in solution.

Both the mono- and bis(pyridine)cobalt(III) species exist in equilibrium over a small range of pyridine–Me_2SO mixtures. An example of the cyclic voltammogram in this transition region is illustrated in Figure 1b. In this region, electrochemical oxidation is of the five-coordinate Me_2SO complex, while the reverse reduction peaks correspond to the simultaneous reduction of both the mono- and bis(pyridine) species. Thus, the reversible oxidation of (p-X)TPPCo(Me_2SO) to yield either (p-X)TPPCo(Me_2SO)(py)$^+$ or (p-X)TPPCo(py)$_2^+$ involves the rapid transfer of an electron before addition of pyridine and the overall electrode reactions may be formulated as shown below. The initial reaction involves the oxidation

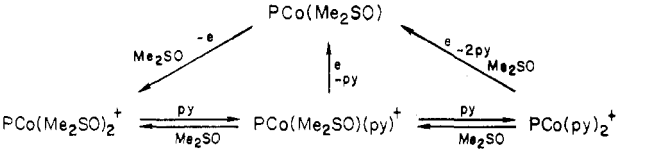

of PCo(Me_2SO), followed by addition of either one or two ligands. The reverse reaction is either via PCo(Me_2SO)(py)$^+$ or PCo(py)$_2^+$, depending on the pyridine concentration. At low concentrations reduction is via the former species (cathodic peak I, Figure 1b) and at high concentrations it is via the latter (cathodic peak II). A slight increase in pyridine shifts the equilibrium toward the bis adduct (log β_2 = 6.4) as final product in the oxidation.

Using eq 2 and the shifts of half-wave potential with pyridine, the complex stoichiometry and formation constants were calculated for addition of pyridine to (p-X)TPPCo-(Me_2SO)$_2^+$ and (p-X)TPPCo(Me_2SO). These data are summarized in Table I. For a comparison with other nonbonding and bonding solvents, we have also calculated the equilibrium constants for addition of pyridine to TPPCo and TPPCo$^+$ in other solvents, as well as for addition of Me_2SO and DMF to TPPCo and TPPCo$^+$ in CH_2Cl_2. These results are shown in Tables II and III.

Table I. Formation Constants for Complexation of Pyridine by (*p*-X)TPPCo and (*p*-X)TPPCo$^+$ in Me_2SO, 0.1 M TBAP

Substituent, X	$4\sigma^a$	Cobalt(III) $\log K_1^b$	Cobalt(III) $\log \beta_2^c$	Cobalt(II) $\log K_1^d$
OCH_3	−1.08	4.15	6.30	1.58
CH_3	−0.68	3.97	6.30	1.47
H	0.00	4.07	6.41	1.32
Cl	0.92	3.97	6.30	1.17
CN	2.64	3.65	6.08	1.15

[a] Reference 21. [b] Reaction: (*p*-X)TPPCo$(Me_2SO)_2^+$ + py ⇄ (*p*-X)TPPCo$(Me_2SO)(py)^+$ + Me_2SO. [c] Reaction: (*p*-X)TPPCo$(Me_2SO)_2^+$ + 2py ⇄ (*p*-X)TPPCo$(py)_2^+$ + $2Me_2SO$. [d] Reaction: (*p*-X)TPPCo(Me_2SO) + py ⇄ (*p*-X)TPPCo(py) + Me_2SO.

Table II. Conditional Stability Constants for Pyridine Complexation by TPPCo$^+$ in Several Solvents

Solvent, S	Dielectric constant[a]	$\log \beta_2^{py}$ (measd)[b]	$\log \beta_2^{S}$ (measd)[c]	$\log \beta_2^{py'}$ (calcd)[d]
CH_2Cl_2	8.93	15.6	nr[g]	15.6
PrCN	20.3	9.1[e,f]		
DMF	36.7	9.1	5.7	14.8
DMA	37.78	10.5[e]		
Me_2SO	46.68	6.4	9.2	15.6
Me_2SO	46.68	5.9[e]	9.2	15.1

[a] Reference 30. [b] Reaction: TPPCo$(S)_2^+$ + 2py ⇄ TPPCo$(py)_2^+$ + 2S. [c] Reaction: TPPCo$^+$ + 2S ⇄ TPPCo$(S)_2^+$. Measurements were made in CH_2Cl_2. [d] $\log \beta_2^{py} = \log \beta_2^{py'}/\beta_2^{S}$; calculated reaction is TPPCo$^+$ + 2py ⇄ TPPCo$(py)_2^+$. [e] Reference 18. [f] Corrected values from ref 18 given in *Anal. Chem.* 48, 456 (1976). [g] No reaction.

Table III. Conditional Stability Constants for Pyridine Complexation by TPPCo in Several Solvents

Solvent, S	Dielectric constant[a]	$\log K_1^{py}$ (measd)[b]	$\log K_1^{S}$ (measd)[c]	$\log K_1^{py'}$ (calcd)[d]
Toluene	2.40	2.88[g]	nr	2.88
CH_2Cl_2	8.93	2.90	nr	2.90
PrCN	20.3	2.60[e,f]		
DMF	36.7	2.07		
DMA	37.78	2.66[e]		
Me_2SO	46.68	2.14[e]	0.63	2.77
Me_2SO	46.68	1.32	0.63	1.95

[a] Reference 30. [b] Reaction: TPPCo(S) + py ⇄ TPPCo(py) + S. [c] Reaction: TPPCo + S ⇄ TPPCo(S). [d] $\log K_1^{py} = \log K_1^{py'}/K_1^{S}$; calculated reaction is TPPCo + py ⇄ TPPCo(py). [e] Reference 18. [f] Corrected values from ref 18 given in *Anal. Chem.*, 48, 456 (1976). [g] Reference 23.

Mechanism of (*p*-X)TPPFeCl Reduction in Me_2SO. In Me_2SO, the cyclic voltammograms consisted of two well-defined reduction peaks corresponding to the reactions Fe(III) ⇌ Fe(II) and Fe(II) ⇌ Fe(I).[5] Monitoring the half-wave potential of Fe(III)/Fe(II) as a function of log (py) yielded a −60 mV slope at low pyridine concentrations and a −120-mV slope at higher pyridine concentrations. This agrees with results in the literature[17] for the unsubstituted complex, TPPFeCl, and can be accounted for by the stepwise addition of pyridine to Fe(II) according to the following reactions:

$$PFe(Me_2SO)_2 + py \overset{K_1}{\rightleftharpoons} PFe(Me_2SO)(py) + Me_2SO \quad (3)$$

$$PFe(Me_2SO)(py) + py \overset{K_2}{\rightleftharpoons} PFe(py)_2 + Me_2SO \quad (4)$$

It has been reported that TPPFe$(Me_2SO)_2^+$ does not bind pyridine.[17] This was verified spectroscopically for all complexes of (*p*-X)TPPFe$(Me_2SO)_2^+$. No changes in visible absorption spectra were observed up to 1.0 M pyridine. Based on these results, the electrode reactions may then be represented as shown in Scheme II.

Scheme II

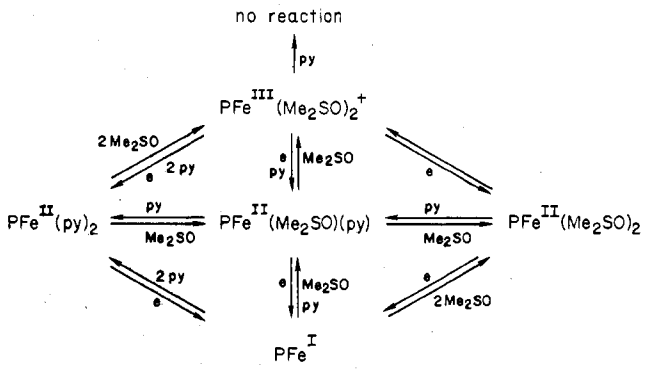

Scheme III

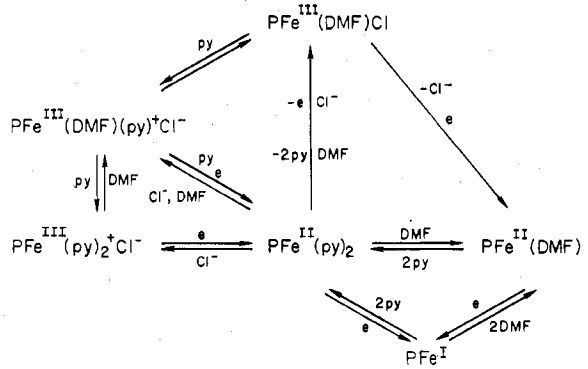

Table IV. Formation Constants for Stepwise Addition of Pyridine to (*p*-X)TPPFe$(Me_2SO)_2$ in Me_2SO, 0.1 M TBAP

Substituent, X	$4\sigma^a$	$\log K_1$	$\log K_2$	$\log \beta_2$
OCH_3	−1.08	2.12	1.00	3.12
OCH_2CH_3	−1.00	1.85	0.89	2.74
CH_3	−0.68	2.20	0.80	3.00
H	0.00	2.44	0.78	3.22
F	0.24	2.22	1.29	3.51
Cl	0.92	1.73	1.27	3.00
Br	0.92	2.27	0.88	3.15

[a] Reference 21.

Stepwise formation constants were measured for reactions 3 and 4, as well as the overall formation constant $\beta_2 = K_1K_2$.

$$PFe(Me_2SO)_2 + 2py \overset{\beta_2}{\rightleftharpoons} PFe(py)_2 + 2Me_2SO \quad (5)$$

The formation constants K_1, K_2, and β_2 for each of the complexes investigated are given in Table IV. The values of ρ calculated from the Hammett plots are tabulated in Table V.

Mechanism of (*p*-X)TPPFeCl Reduction in DMF. The reduction of iron porphyrins in DMF is complex and has been the subject of several studies.[14,16,17] Overall, the electrode reactions of (*p*-X)TPPFeCl in DMF–pyridine mixtures may be represented as shown in Scheme III.

The initial PFe(DMF)Cl is extremely stable and will bind with pyridine only at high ligand concentrations. Even at 1.0 M pyridine, most of the iron(III) is still uncomplexed by pyridine. Reduction of PFe(DMF)Cl yields first $PFe^{II}(DMF)$, followed by a rapid transfer of two pyridine molecules to form $PFe^{II}(py)_2$. This complex can then be reoxidized to yield either $Fe^{III}(DMF)Cl$ or one of two iron(III) pyridine complexes. In DMF both mono- and bis(pyridine) adducts are observed with iron(III). In contrast, iron(II) forms only the bis(pyridine) complex indicating that $K_2 >> K_1$. This several orders of magnitude difference in formation constants is not observed in Me_2SO (see Table IV), where $K_2 < K_1$, and both the mono-

Table V. Summary of Hammett Reaction Constants, ρ, for Several Complexes of Cobalt(III), Cobalt(II), Iron(III), and Iron(II) Para-Substituted Tetraphenylporphyrins

Metal	Solvent	Axial ligand	ρK_1[a]	ρK_2[b]	$\rho\beta_2$[c]	Ref
Fe(III)	$CHCl_3$	*N*-CH_3Im			−0.39	12
	$CHCl_3$	*N*-CH_3Im			−0.41	13
	DMF	py	−0.45	0.02	−0.43	14, tw[d]
Fe(II)	DMF	py			0.13	14
	Me_2SO	py	0.04	0.05	0.09	tw[d]
Co(III)	Me_2SO	py	0.0	0.0	0.0	tw[d]
Co(II)	Toluene	pip	0.145	nr[d]	nr[d]	3
	Toluene	py	0.168	nr[d]	nr[d]	3
	Me_2SO	py	−0.16	nr[d]	nr[d]	tw[d]

[a] ρ for stepwise addition of first nitrogenous base. [b] ρ for stepwise addition of second nitrogenous base. [c] ρ for overall addition of two nitrogeneous bases. [d] Key: nr = no reaction, tw = this work.

and bis(pyridine) complex may be isolated.

Linear free energy plots as described by eq 1 were constructed for both the mono- and bis(pyridine) adducts with iron(III) in DMF.

$$PFe(DMF)Cl + py \overset{K_1}{\rightleftharpoons} PFe(py)(DMF)^+Cl^- \quad (6)$$
$$\rho = -0.45$$

$$PFe(DMF)Cl + 2py \overset{\beta_2}{\rightleftharpoons} PFe(py)_2^+Cl^- + DMF \quad (7)$$
$$\rho = -0.43$$

Combining reactions 6 and 7 yields the formation constant for addition of a second pyridine to the mono(pyridine) complex

$$PFe(DMF)(py)^+Cl^- + py \overset{K_2}{\rightleftharpoons} PFe(py)_2^+Cl^- + DMF \quad (8)$$

where $K_2 = \beta_2/K_1$. Linear free energy plots of K_1, K_2, and β_2 are shown in Figure 3 and the calculated reaction constants are tabulated in Table V.

Discussion

Effect of Solvent on Formation Constants for Pyridine Binding to TPPCo and TPPCo$^+$. Previous studies concerning the effect of solvent on reactions of iron and cobalt porphyrins have led to the conclusion that ΔG (or log K_{eq}) was strongly dependent on solvent.[12,17,18,24-27] Walker et al.[12] has observed that both K_1 and β_2 for *N*-methylimidazole complexes with iron(III) increase with increase in the solvent polarity and has related the log K_1 and log β_2 linearly with the solvent polarity parameter E_T. However, in solvents of high polarity, one would predict a decrease in the apparent formation constant due to solvent competition for the axial coordination position on the porphyrin metal. In bonding solvents, stability constants calculated for ligand addition to metalloporphyrins are actually "conditional formation constants"[28] involving displacement of the bound solvent molecule by another axial ligand. In these cases, the dissociation constant of the solvent–metalloporphyrin complex and the formation constant of the ligand–metalloporphyrin complex must each be considered.

The axial displacement of solvent by pyridine

$$TPPCo(S)_2^+ + 2py \overset{\beta_2^{py}}{\rightleftharpoons} TPPCo(py)_2^+ + 2S \quad (9)$$

may be considered mathematically as occurring in two steps; first dissociation of the solvent and then binding of the ligand

$$TPPCo(S)_2^+ \overset{1/\beta_2^S}{\rightleftharpoons} TPPCo^+ + 2S \quad (10)$$

$$TPPCo^+ + 2py \overset{\beta_2^{py'}}{\rightleftharpoons} TPPCo(py)_2^+ \quad (11)$$

where $1/\beta_2^S$ is the dissociation constant of the solvent, S, β_2^{py} is the conditional formation constant for pyridine addition, and $\beta_2^{py'}$ is the actual formation constant that would be obtained if the solvent were totally dissociated from the complex. The overall measured stability constant may be expressed as

$$\beta_2^{py} = \beta_2^{py'}/\beta_2^S$$

Similar equations are derived for the complexation of the five-coordinate complexes of Co(II). The relevant formation constants are K_1^{py}, $K_1^{py'}$, and K_1^S.

In Tables II and III are listed the measured values of β_2^S and K_1^S for Me_2SO and DMF binding to TPPCo$^+$ and TPPCo in the noncomplexing solvent CH_2Cl_2. Using these values we have calculated the hypothetical $\beta_2^{py'}$ and $K_1^{py'}$ which might be obtained for TPPCo$^+$ and TPPCo complexation by pyridine in the polar solvents DMF and Me_2SO. Although the calculations are approximate and we have neglected solvent–solute interactions, there is agreement between the values of log $\beta_2^{py'} \approx 15$ obtained in different solvents for $TPPCo(py)_2^+$ formation and log $K_1^{py'} \approx 3$ for TPPCo(py) formation.

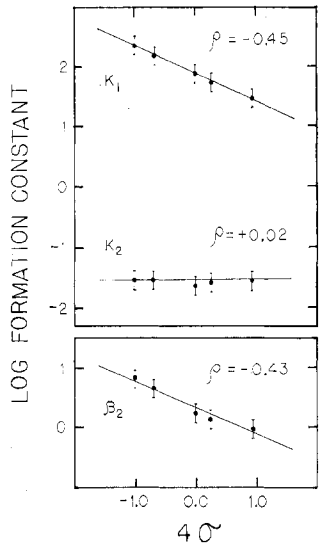

Figure 3. Linear free energy plot of log K_1, log K_2, and log β_2 vs. 4σ for pyridine binding of TPPFeCl in DMF, 0.1 M TBAP.

Effect of Solvent and Metal Oxidation State on Substituent Effects. In Table V are listed the values of ρ for the para-substituted cobalt and iron tetraphenylporphyrins. Plots of β_2 and K_1 vs. 4σ give a negative slope for reactions of iron(III), while for similar reactions of Fe(II) and Co(III), ρ is positive or zero. For bis ligand complexation of (*p*-X)TPPFeCl a negative Hammett ρ indicates that electron-donating substituents favor the reaction. The reverse trend from all other +2 metalloporphyrins[3,10,11,14] has been interpreted as due to stabilization of the positive charge on the ferric iron by electron-donating groups and has been discussed in detail by Walker et al.[12] It is interesting to note that for (*p*-X)TPPFeCl an almost identical ρ is obtained by electrochemical methodologies[14] as by NMR techniques[13] and by optical titrations[12] despite the change between pyridine and *N*-methylimidazole as axial ligands.

When considering substituent effects of the oxidized and reduced iron and cobalt porphyrins, it appears that the magnitude of ρ for ligand addition does not significantly depend on the charge of the metal ion as has been suggested in previous studies.[3,14] Addition of pyridine to the positively charged (*p*-X)TPPCo$(Me_2SO)_2^+$ yields K_1 and β_2 (Table I) which, unlike (*p*-X)TPPFe$^+$, are independent of the nature of the electron-donating/-withdrawing characteristics of the substituent. However, as mentioned above, the experimentally measured stability constants involve a solvent displacement reaction at the axial coordination positions. It may be that

ρ for complexation of (*p*-X)TPPCo$^+$ with Me_2SO exactly balances ρ for pyridine complexation with (*p*-X)TPPCo$^+$ and the overall result is a zero slope in the plot of log β_2 vs. 4σ. Likewise, the $\rho = -0.16$ for TPPCo(py) formation in Me_2SO, when compared to $\rho = 0.16$ in toluene, might be explained by the presence, on the initial reactant, of a bound Me_2SO molecule which is more strongly affected by ring substituents than is the axially bound pyridine in the product. Another plausible explanation is that the oxidized product is not ion paired in Me_2SO and that the complex exists as the positively charged $PCo(Me_2SO)_2^+$. A similar dissociated $PFe(Me_2SO)_2^+$ exists in solution when PFeCl is dissolved in Me_2SO.[29] Furthermore, in the case of the oxidized PCo, the only anion in solution is the weakly binding ClO_4^- which will not strongly associate with cobalt(III).

With iron tetraphenylporphyrin, two points are especially of interest. The first is that for pyridine complexation by (*p*-X)TPPFeCl in DMF, $K_2 << K_1$. This is opposite the order observed in the nonbonding solvent $CHCl_3$ where $K_2 >> K_1$ and might be accounted for by a change in ion pair association or a change in spin state from high-spin iron(III) in (*p*-X)-TPPFe(DMF)Cl to low-spin iron(III) in the mono(pyridine) adduct. Indeed, shifts of 500 mV in $E_{1/2}$ and the noncoupled oxidation–reduction observed in DMF[14] strongly support either of these changes.

The second point of interest is that K_2 is apparently independent of the nature of the substituent (see Figure 3). For addition of the first pyridine molecule to TPPFe(DMF)Cl, the plot of log K_1 vs. 4σ is negative ($\rho = -0.45$) presumably due to stabilization of the iron(III) in an ion-paired product.[12] On the other hand, if addition of the second pyridine molecule is postulated to yield $TPPFe(py)_2^+Cl^-$, the reaction would involve an ion-paired reactant and an ion-paired product (see Scheme III). In this case, it might be predicted that a large negative ρ would not be obtained since, unlike the overall reaction in $CHCl_3$ or DMF, the reactant would already be ion paired and an equal stabilization of product and reactant would occur. Plots of log K_2 vs. 4σ gave a $\rho = 0.02$ (Figure 3).

Further work on ion pairing and ligand addition reactions of other positively and negatively charged metalloporphyrin complexes is now in progress. Results of substituent effects for axial ligand addition in bonding and nonbonding solvents should help to elucidate the effects which influence the transmission of electron density from the porphyrin ring to the central metal and determine both the magnitude of the formation constants and the sign of ρ.

Acknowledgment. Support of this work by the Robert A. Welch Foundation, Research Corporation, and the New Research Opportunities Program (NROP) from the University of Houston is gratefully acknowledged.

Registry No. (*p*-OCH_3)TPPCo$(Me_2SO)_2^+$, 65832-38-4; (*p*-OCH_3)TPPCo$(Me_2SO)(py)^+$, 65832-39-5; (*p*-CH_3)TPPCo-$(Me_2SO)_2^+$, 65832-40-8; (*p*-CH_3)TPPCo$(Me_2SO)(py)^+$, 65832-41-9; TPPCo$(Me_2SO)_2^+$, 65832-42-0; TPPCo$(Me_2SO)(py)^+$, 65832-43-1; (*p*-Cl)TPPCo$(Me_2SO)_2^+$, 65832-44-2; (*p*-Cl)TPPCo$(Me_2SO)(py)^+$, 65890-15-5; (*p*-CN)TPPCo$(Me_2SO)_2^+$, 65832-45-3; (*p*-CN)-TPPCo$(Me_2SO)(py)^+$, 65832-46-4; (*p*-OCH_3)TPPCo$(py)_2^+$, 65832-47-5; (*p*-CH_3)TPPCo$(py)_2^+$, 65832-48-6; TPPCo$(py)_2^+$, 47902-90-9; (*p*-Cl)TPPCo$(py)_2^+$, 65832-49-7; (*p*-CN)TPPCo$(py)_2^+$, 65832-50-0; (*p*-OCH_3)TPPCo(Me_2SO), 65832-51-1; (*p*-OCH_3)-TPPCo(py), 41736-30-5; (*p*-CH_3)TPPCo(Me_2SO), 65832-52-2; (*p*-CH_3)TPPCo(py), 60470-23-7; TPPCo(Me_2SO), 65832-53-3; TPPCo(py), 29130-61-8; (*p*-Cl)TPPCo(Me_2SO), 65832-54-4; (*p*-Cl)TPPCo(py), 60430-16-2; (*p*-CN)TPPCo(Me_2SO), 65832-55-5; (*p*-CN)TPPCo(py), 60430-17-3; TPPCo$(PrCN)_2$, 65832-56-6; TPPCo$(DMF)_2$, 65832-57-7; TPPCo$(DMA)_2$, 65832-58-8; TPPCo, 14172-90-8; TPPCo(PrCN), 65832-61-3; TPPCo(DMF), 65832-62-4; TPPCo(DMA), 65832-63-5; (*p*-OCH_3)TPPFe$(Me_2SO)_2$, 65832-64-6; (*p*-OCH_3)TPPFe$(Me_2SO)(py)$, 65890-16-6; (*p*-OCH_2CH_3)-TPPFe$(Me_2SO)_2$, 65832-65-7; (*p*-OCH_2CH_3)TPPFe$(Me_2SO)(py)$, 65832-66-8; (*p*-CH_3)TPPFe$(Me_2SO)_2$, 65832-59-9; (*p*-CH_3)-TPPFe$(Me_2SO)(py)$, 65832-60-2; TPPFe$(Me_2SO)_2$, 65832-68-0; TPPFe$(Me_2SO)(py)$, 65832-69-1; (*p*-F)TPPFe$(Me_2SO)_2$, 65832-70-4; (*p*-F)TPPFe$(Me_2SO)(py)$, 65832-71-5; (*p*-Cl)TPPFe$(Me_2SO)_2$, 65832-72-6; (*p*-Cl)TPPFe$(Me_2SO)(py)$, 65890-14-4; (*p*-Br)-TPPFe$(Me_2SO)_2$, 65832-73-7; (*p*-Br)TPPFe$(Me_2SO)(py)$, 65890-17-7; (*p*-OCH_3)TPPFe$(py)_2$, 50914-95-9; (*p*-OCH_2CH_3)TPPFe$(py)_2$, 65832-67-9; (*p*-CH_3)TPPFe$(py)_2$, 62612-73-1; TPPFe$(py)_2$, 16999-25-0; (*p*-F)TPPFe$(py)_2$, 60250-90-0; (*p*-Cl)TPPFe$(py)_2$, 50914-74-4; (*p*-Br)TPPFe$(py)_2$, 65832-82-8; TPPFeCl, 16456-81-8.

References and Notes

(1) (a) University of Houston. (b) Robert A. Welch Predoctoral Fellow.
(2) (a) K. M. Kadish and M. M. Morrison, *J. Am. Chem. Soc.*, **98**, 3326 (1976); (b) *Inorg. Chem.*, **15**, 980 (1976); (c) *Bioinorg. Chem.*, **7**, I07 (1977).
(3) F. A. Walker, D. Beroiz, and K. M. Kadish, *J. Am. Chem. Soc.*, **98**, 3484 (1976).
(4) H. J. Callot, A. Giraudeau, and M. Gross, *J. Chem. Soc., Perkin Trans. 2*, 1321 (1975).
(5) K. M. Kadish, M. M. Morrison, L. A. Constant, L. Dickens, and D. G. Davis, *J. Am. Chem. Soc.*, **98**, 8387 (1976).
(6) (a) M. Meot-Ner and A. D. Adler, *J. Am. Chem. Soc.*, **94**, 4764 (1972); (b) *ibid.*, **97**, 5107 (1975).
(7) (a) S. S. Eaton and G. R. Eaton, *J. Am. Chem. Soc.*, **97**, 3660 (1975); (b) *Inorg. Chem.*, **16**, 72 (1977).
(8) E. W. Baker, C. B. Storm, G. T. McGrew, and A. H. Corwin, *Bioinorg. Chem.*, **3**, 49 (1973).
(9) B. D. McLees and W. S. Caughey, *Biochemistry*, **7**, 642 (1968).
(10) F. A. Walker, E. Hui, and J. M. Walker, *J. Am. Chem. Soc.*, **97**, 2390 (1975).
(11) G. C. Vogel and B. A. Beckmann, *Inorg. Chem.*, **15**, 483 (1976).
(12) F. A. Walker, M-W. Lo, and M. T. Ree, *J. Am. Chem. Soc.*, **98**, 5542 (1976).
(13) J. D. Satterlee, G. N. La Mar, and J. S. Frye, *J. Am. Chem. Soc.*, **98**, 7275 (1976).
(14) K. M. Kadish and L. A. Bottomley, *J. Am. Chem. Soc.*, **99**, 2380 (1977).
(15) J. E. Leffler and E. Grunwald, "Rates and Equilibria of Organic Reactions", Wiley, New York, N.Y., 1963, pp 172–179.
(16) J. Manassen, *Isr. J. Chem.*, **12**, 1959 (1974).
(17) L. A. Constant and D. G. Davis, *Anal. Chem.*, **47**, 2253 (1975).
(18) L. A. Truxillo and D. G. Davis, *Anal. Chem.*, **47**, 2260 (1975).
(19) I. M. Kolthoff and J. J. Lingane, "Polarography", 2nd ed, Vol. I, Interscience, New York, N.Y., 1952, p 66.
(20) (a) A. D. Adler, F. R. Longo, J. D. Finarelli, J. Goldmacher, J. Assour, and L. Korsakoff, *J. Org. Chem.*, **32**, 476 (1967); (b) A. D. Adler, F. R. Longo, F. Kampas, and J. Kim, *J. Inorg. Nucl. Chem.*, **32**, 2443 (1970).
(21) H. H. Jaffe, *Chem. Rev.*, **53**, 191 (1953).
(22) R. S. Nicholson and I. Shain, *Anal. Chem.*, **36**, 706 (1964).
(23) F. A. Walker, *J. Am. Chem. Soc.*, **95**, 1150 (1973).
(24) (a) H. C. Stynes and J. A. Ibers, *J. Am. Chem. Soc.*, **94**, 1559 (1972); (b) D. V. Stynes, H. C. Stynes, B. R. James, and J. A. Ibers, *ibid.*, **95**, 1796 (1973).
(25) (a) S. J. Cole, G. C. Curthoys, and E. A. Magnusson, *J. Am. Chem. Soc.*, **92**, 2991 (1970); (b) *ibid.*, **93**, 2153 (1971).
(26) D. Brault and M. Rougee, *Biochemistry*, **13**, 4551 (1974).
(27) H. Goff and L. O. Morgan, *Inorg. Chem.*, **15**, 2069 (1976).
(28) J. Inczedy, "Analytical Applications of Complex Equilibria", Ellis Horwood Ltd., Westergate, England, 1976.
(29) S. B. Brown and I. R. Lantzke, *Biochem. J.*, **115**, 279 (1969).
(30) D. T. Sawyer and J. C. Roberts, "Experimental Electrochemistry for Chemists", Wiley, New York, N.Y., 1974.